AN ANOMALY CLOCK DETECTION ALGORITHM FOR A ROBUST CLOCK ENSEMBLE

Qinghua Wang and Pascal Rochat
SpectraTime
Vauseyon 29, 2000 Neuchâtel, Switzerland
Tel: +41 32 732 16 66, Fax: +41 32 732 16 67
E-mail: *qinghua@spectratime.com, rochat@spectratime.com*

Abstract

The Anomaly Clock Detection Algorithm is intended to facilitate a monitoring system to better manage a clock system, insuring continuity of operations and limiting the expected degradation of performance due to contingencies and anomalies.

A novel ensemble of five Rubidium Atomic Frequency Standards (RAFS) is proposed onboard the future Global Navigation Satellite System. All clocks are in phase and on frequency all the time with advantages of relatively simple, robust, fully redundant, and improved performance. It allows reliable anomaly detection and smooth switch-over of master and redundant clocks using the same clock model.

The algorithm is designed on the basis of the clock output phase/frequency measurements to detect the 'Feared Events' such as phase jump, frequency jump, and frequency instability, which affect various atomic clocks.

The proper detection strategy has been determined in view of the detection capability and computation efforts. Algorithm parameters, such as the sliding window width as a function of the time constant, and the minimum detectable levels have been optimized and verified as the trade-off of the detection capability, response speed, and detection confidence. The verification results under numerous test cases in the presence of anomalies that occurred in various RAFS, as well as the clock ensemble, are demonstrated.

I. INTRODUCTION

A novel 'onboard clock ensemble' is proposed for the clock monitoring and control configuration of the future Global Navigation Satellite System (GNSS).

Figure 1 shows a possible configuration constituted by a 'new Rubidium Atomic Frequency Standard (RAFS)' equipped with a synthesizer, a multi-channel phase comparator, and controller/algorithms. The minimum number of RAFS powered shall be at least three units in order to be able to perform clock anomaly detections and automatic switch-over. This system could also run with four or five units operating at one time, and perform corrections of the master clock, which is connected to the navigation payload in function of the 'weighted' average of the 'Phase-Locked Loop' clock ensemble.

This clock ensemble shall offer very robust solutions, high reliability, autonomous integrity monitoring, redundancy, and improved performance. All clocks are 'in phase' and 'on frequency' all the time. Since

the smooth switch-over of defective or unstable clocks of the ensemble could be made without the upload of new clock model, this solution will keep the satellite operational in any conditions of clock anomalies.

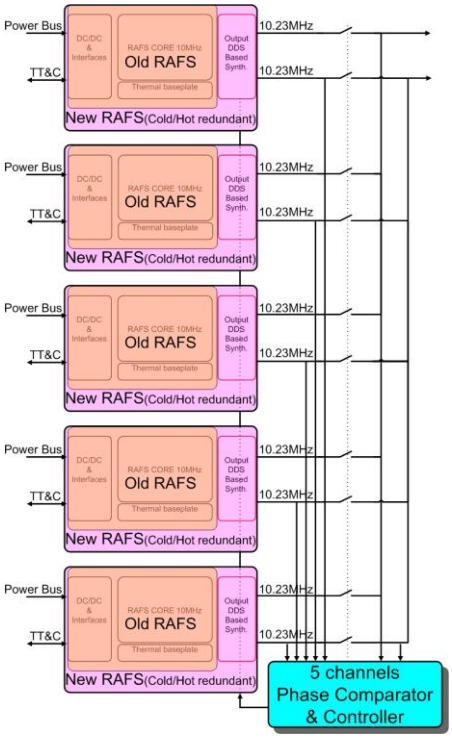

Figure 1. Proposed onboard clock ensemble.

To assure reliable clock anomalies detection, we are developing the Anomaly Clock Detection Algorithm for space RAFSs.

II. ARCHITECTURE OF THE ANOMALY CLOCK DETECTION ALGORITHM

Figure 2 shows the architecture of the Anomaly Clock Detection Algorithm. The algorithm is designed on the basis of the clock output phase measurements via the multi-channel phase comparator to detect the 'Feared Events' as phase jump, frequency jump, and frequency instability, which affect the performance of clocks.

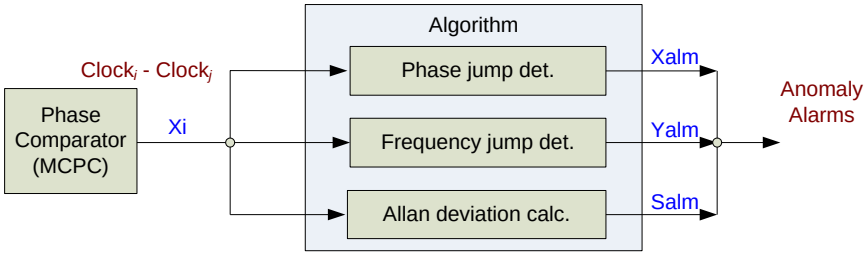

Figure 2. Architecture of the Anomaly Clock Detection Algorithm.

The frequency stability performance is characterized by the two-sample variance without dead time (i.e. Allan variance), with the well-known defined equation. This is not particularly addressed in this paper.

In the following, we discuss the proper detection strategy selection and optimize the algorithm parameters such as time constant, window width, and minimum detection level. The RAFS raw data are generated for these simulations with the noise parameters as white FM of $5\times10^{-12}\tau^{-1/2}$, flicker FM of 3×10^{-14}, and frequency drift of $1\times10^{-12}/day$.

In addition, the algorithm operability verification under real test cases in presence of jumps in individual RAFSs and the clock ensemble are presented.

III. PROPER DETECTION STRATEGY SELECTION

Figure 3 illustrates the block diagram of the phase or frequency jump detector. Two strategies have been studied for the phase/frequency jump detection: the least-squares linear fitting and the standard deviation.

- LSLF refers to the strategy computing the deviation of the real data from the Least Squares Linear Fitting of the previous data sequence in sliding windows.

- StdDev refers to the strategy computing the classical variance (standard deviation) of the data sequence in sliding windows.

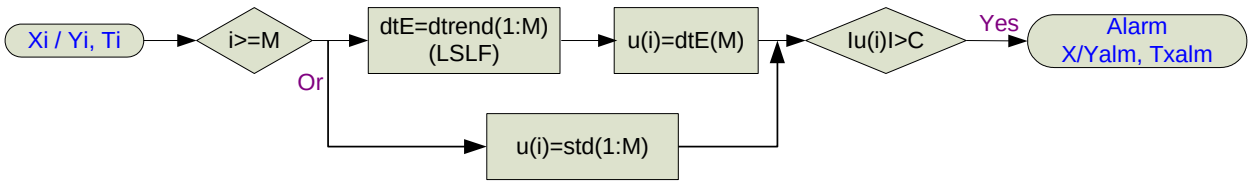

Figure 3. Block diagram of the phase or frequency jump detector.

The input phase or frequency data (Xi or Yi) at the averaging time Ti (or time constant) are calculated over the previous M data in sliding window. If the absolute value exceeds the outlier criterion C, an Alarm is generated.

Abbreviations are used as below:

Tau_ph : phase time constant
Len_ph : sliding window width on phase deviation calculation
Tau_fr : frequency time constant
Len_fr : sliding window width on frequency deviation calculation.

Figure 4 compares the results by LSLF and StdDev for phase jump detection. It shows that the ratio of the anomaly-caused phase deviation over the max normal value is higher by LSLF, and the anomaly is hidden within the noise of the normal phase standard deviation. For the small time constant and the window width, the computation efforts advantage of StdDev is not significant.

Therefore, the strategy of LSLF appears a proper alternative for the phase jump detection in the view of the detection capability with the trade-off of the solution time.

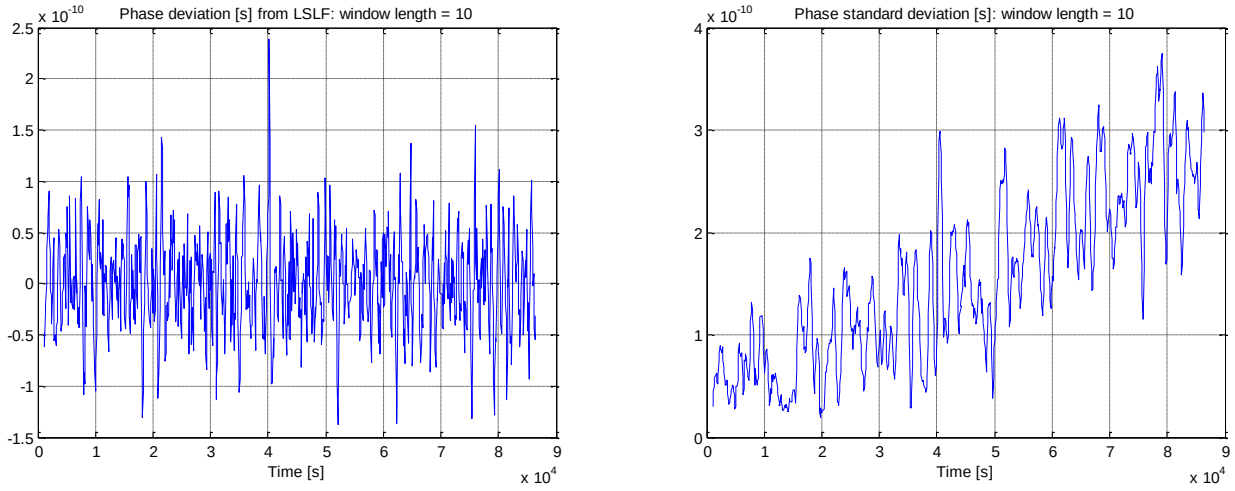

Figure 4. Comparison of test results by strategies of LSLF and StdDev for phase jumps of 350ps @ 40,000 s by a RAFS (with tau_ph = 100 s, len_ph = 10).

The comparison of LSLF and StdDev for frequency jump detection (Figure 5) shows that the ratio of the anomaly-caused frequency deviation over the max normal value is higher by StdDev. And LSLF involves heavier computation, especially when the bigger time constant and the window width are required.

Therefore, the strategy of StdDev appears a proper alternative for the frequency jump detection in view of the detection capability and computation efforts, although the direction (sign) of the jump cannot be identified.

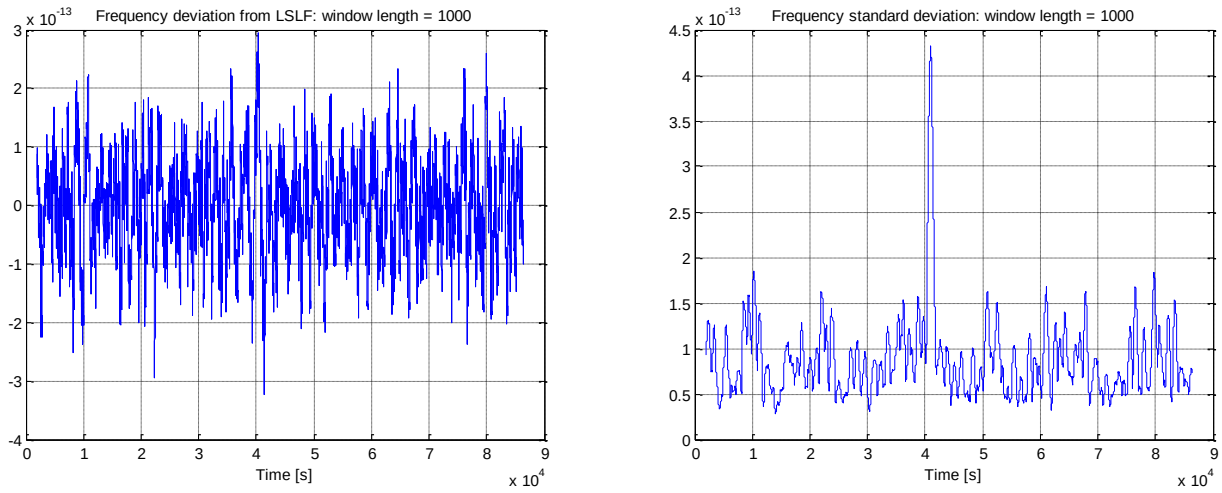

Figure 5. Comparison of test results by strategies of LSLF and StdDev for the frequency jump of 1.5×10^{-12} @ 40,000 s by a RAFS with len_fr = 1000 (tau_fr = 1000 s).

IV. ALGORITHM PARAMETER OPTIMIZATION

For the phase jump detection, the time constant tau_ph is selected as 100 s, which allows the measurement system noise to be much lower than the space RAFS noise.

Figure 6 compares the sliding window widths (len_ph) for the phase jump detection by LSLF, with results for len_ph = 5, 10, and 100 for a jump of 500 ps @ 40,000 s on a RAFS (tau_ph = 100 s).

It shows that the wider window might hide a small phase jump. The base level of the phase deviation without affected by the jump is higher with the wider window. This effect is understandable, since the RMS of the time with regards to Allan deviation is $\sigma_x(\tau) = \sigma_y(\tau) \cdot \tau$, $\sigma_x(\tau) \propto \sqrt{\tau}$ when the white frequency noise is dominant.

Ratios of the peak phase deviation caused by the jump over normal values are similar for len_ph = 5 and 10. However, len_ph = 10 is selected with higher confidence for the data fitting.

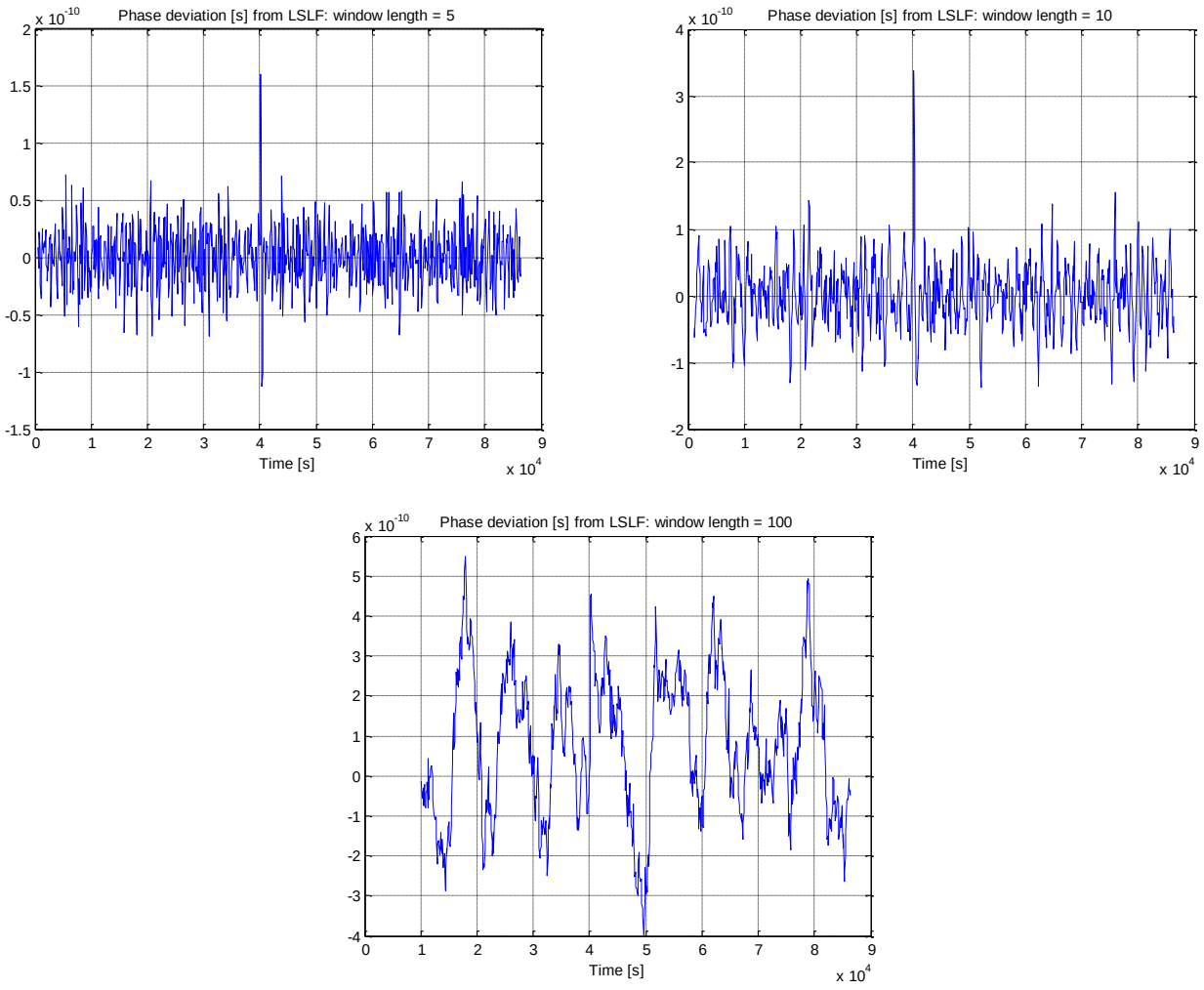

Figure 6. Comparison of test results for len_ph = 5, 10, and 100 by LSLF for the phase jump of 500 ps @ 40,000 s by a RAFS (tau_ph = 100 s).

Figure 7 compares the sliding window widths (len_fr) for the frequency jump detection by StdDev, with results for len_fr <, =, and > tau_fr for a jump of 1×10^{-12} @ 40,000 s on a RAFS. The time constant tau_fr has been determined to be 1000 s in order to detect such a level of frequency jump.

It shows that the ratio of the peak frequency deviation caused by the jump over normal values is higher with the wider window size. However, the wider window leads to the slower response and heavier computation.

As the trade-off of the detection capability, response speed, and computation efforts, the parameter of len_fr is optimized equal to tau_fr, i.e. len_fr = 1000.

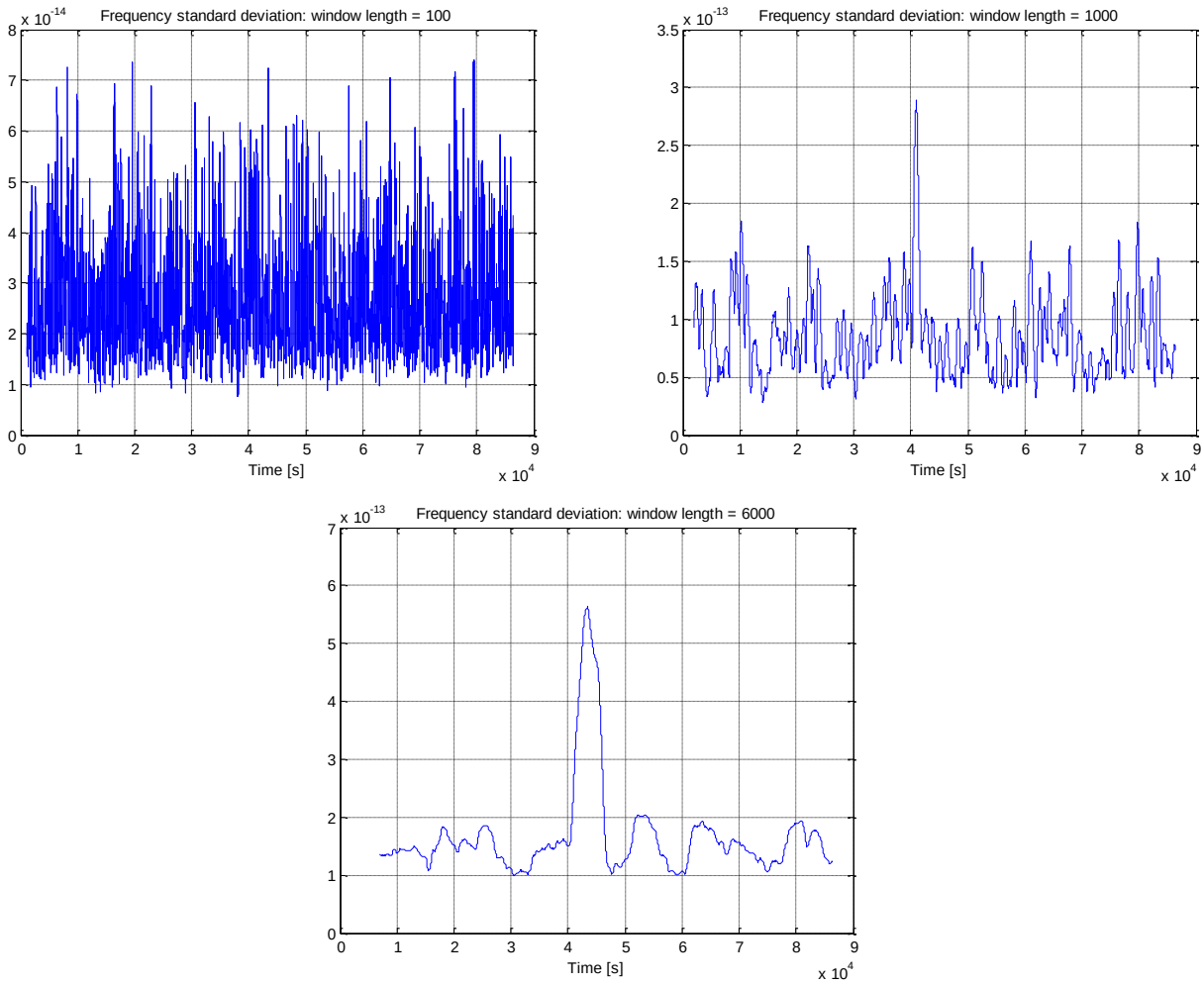

Figure 7. Comparison of test results for len_fr <, =, and > tau_fr (1000 s) by StdDev for the frequency jumps of 1×10^{-12} @ 40,000 s by a RAFS.

V. ALGORITHM VERIFICATION

By means of the selected jump strategy with optimum algorithm parameters, simulations under numerous test cases have been performed to verify the algorithm operability.

For this purpose, real measurement data (Figure 8) during 1 month from five individual RAFS with various behaviors in terms of frequency jump, drift, and stability were analyzed.

As described earlier, these five RAFS constitute a clock ensemble, in which frequencies of all five clocks can be corrected into one weighted and jump removed 'ensemble' frequency. The clock ensemble output is also analyzed to compare the results of individual RAFSs.

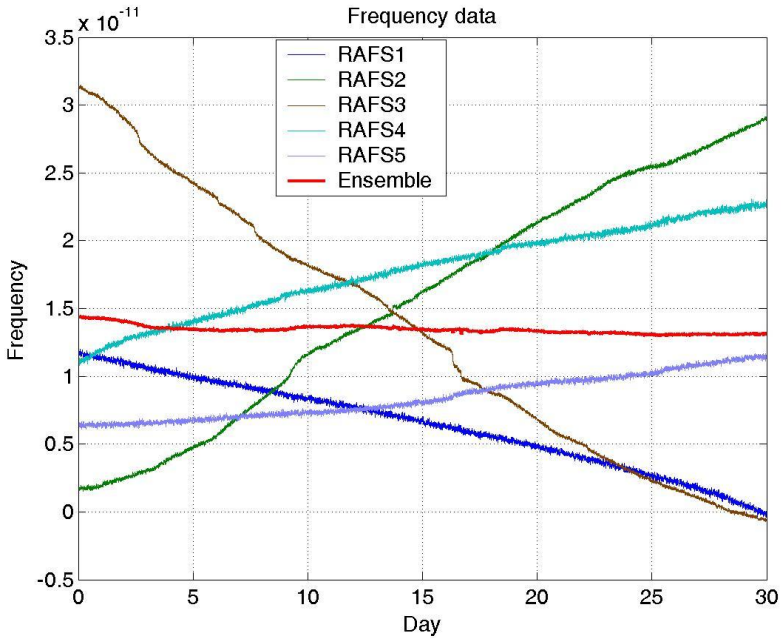

Figure 8. Frequency data for five individual RAFSs and clock ensemble (initialized).

Figure 9 shows the frequency standard deviation by frequency jump detection. A detection threshold is determined in order to detect the minimum frequency jump amplitude of 2.5×10^{-13}. The baseline threshold is the trade-off between minimum detectable level and maximum confidence.

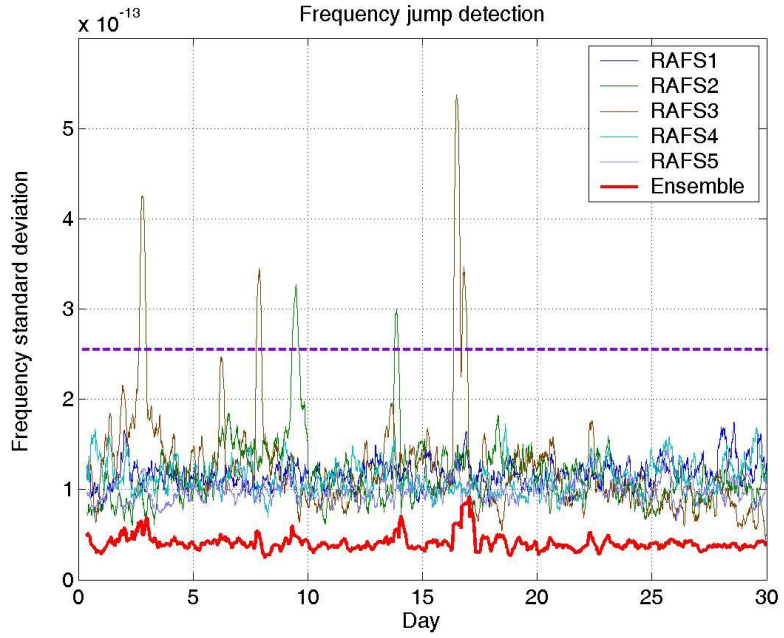

Figure 9. Frequency jump detection for five individual RAFSs and clock ensemble.

It demonstrates that all frequency jumps are detected correctly by the algorithm, and the total number of six jumps with amplitude from 7×10^{-13} to 3×10^{-13} for five RAFS is eliminated in the clock ensemble whose maximum amplitude is only 1×10^{-13}.

Figure 10 shows the comparison of the frequency stability. The short-term frequency stability of the clock ensemble is optimized due to the weighting function according to the short-term stabilities of all five individual RAFSs, and the ensemble stability near 10,000 s is further improved due to the frequency jump removal.

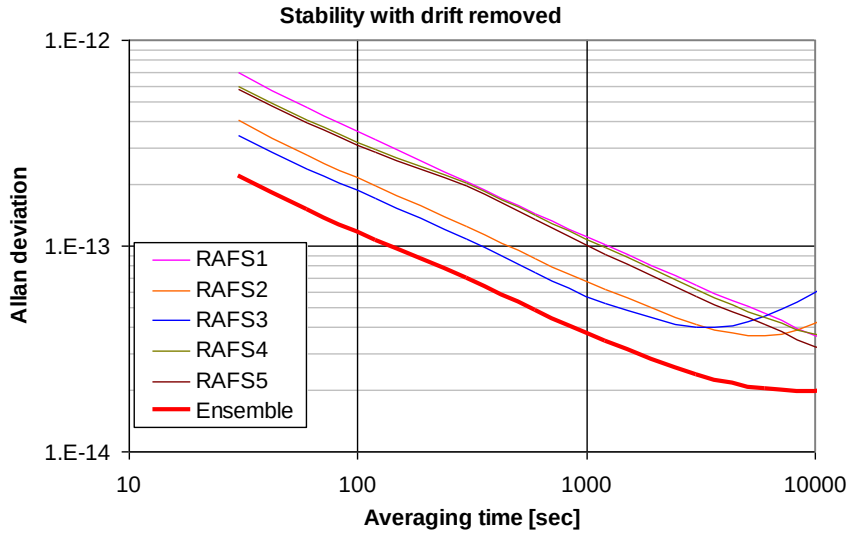

Figure 10. Frequency stability for five individual RAFSs and clock ensemble.

VI. CONCLUSIONS

The Anomaly Clock Detection Algorithm for a robust onboard clock ensemble has been developed with appropriate strategies and optimized algorithm parameters.

The algorithm operability is verified under real test cases with five individual RAFS and the clock ensemble.

The clock ensemble demonstrates significant advantages from an individual RAFS, in terms of reduced frequency jump, improved frequency stability, and frequency drift.